

# Using PhreePlot to Calibrate Mining Related Geochemical Models: A User's Perspective

**John Mahoney**

*Mahoney Geochemical Consulting, USA*

## ABSTRACT

With the release of the program PhreePlot, geochemists obtained a method to better understand and quantify geochemical processes. PhreePlot's ability to optimize a wide range of parameters in PHREEQC based models provides a simple and direct method to better calibrate geochemical models. In its fitting routines, PhreePlot calculates the weighted residual sum of squares [W(RSS)] between the measured (observed) and modeled data. The optimization routine minimizes this value by changing user defined variables in the attached PHREEQC model. The combination of several fitting options, plus flexibilities inherent in PHREEQC, allows for a range of approaches in quantitative geochemical data evaluation. The simplest applications permit straightforward fitting of experimental or field measurements for solubility product calculations. The fitting of surface complexation reactions over a large range of experimental conditions is another straightforward application. Many parameters in PHREEQC such as surface site densities, and rate constants are suitable for fitting and can be used to match measured data with modeled results. The quantitative understanding from these rigorous fits can produce stronger insights about the geochemical processes and potentially simplify regulatory reviews.

**Keywords:** PHREEQC, PhreePlot, Model optimization, Arsenic, Surface complexation

## INTRODUCTION

The program PhreePlot (Kinniburgh and Cooper 2011) uses PHREEQC (Parkhurst and Appelo 2013) to prepare a wide variety of figures including species distribution plots, Eh-pH diagrams, and other types of activity - activity plots. To construct these figures, PhreePlot cycles through a range of user defined conditions such as pH, oxygen fugacities or pe, and component concentrations. Numerous options are available to make these figures and even animations can be prepared using the Hunt and Track method (Kinniburgh and Cooper 2004) to define the Eh-pH conditions, and a separate looping option to set a range of concentrations (see PhreePlot Website). Because it uses a large thermodynamic database the figures are more accurate than the simpler plots described in many textbooks and references.

The ability to change a “tagged” parameter(s) provides a means to optimize selected parameters through the fitting routine. There are several fitting options in PhreePlot, and it is this capability that is described below. In the current PhreePlot user’s guide there are a limited number of fitting examples. The following describes a range of applications and efforts to learn how to prepare optimized geochemical models.

A comment about program installation is appropriate. Although installation of PhreePlot and its two supporting programs GPL Ghostscript and GSview appears daunting, it is straightforward. The key issue I have run into is to make sure that the path to the pdf maker is correctly listed in the pp.set file.

## COMPARISON OF PhreePlot TO UCODE\_2005

Before PhreePlot was released in 2011 one optimization method that was commonly employed was to couple a batch version of PHREEQC with UCODE\_2005 (Poeter et al. 2005). Mahoney et al. (2009) used such an approach to fit four uranyl surface complexation constants onto the hydrous ferric oxide (HFO) surface. It was decided that these data sets and models would provide a reasonably straightforward test of PhreePlot capabilities. Both UCODE and PhreePlot use a similar method to “tag” the adjustable parameters and to tabulate observations. Consequently, the original batch PHREEQC input files and observation data files required little updating to accommodate the PhreePlot requirements. The same order of fitting the constants as described in Mahoney et al. (2009) was used. The  $K_1^{int}$  and  $K_2^{int}$  values were first fit using carbonate free experimental data, and then  $K_3^{int}$  was fit and finally the  $K_4^{int}$  value was fit. PhreePlot calculated the essentially same log  $K^{int}$  values (Table 1) reported in Mahoney et al. (2009).

**Table 1** Comparison of batch PHREEQC/UCODE\_2005 values of surface complexation constants to values estimated using PhreePlot, the NEA database for uranyl complexes was used in all calculations.

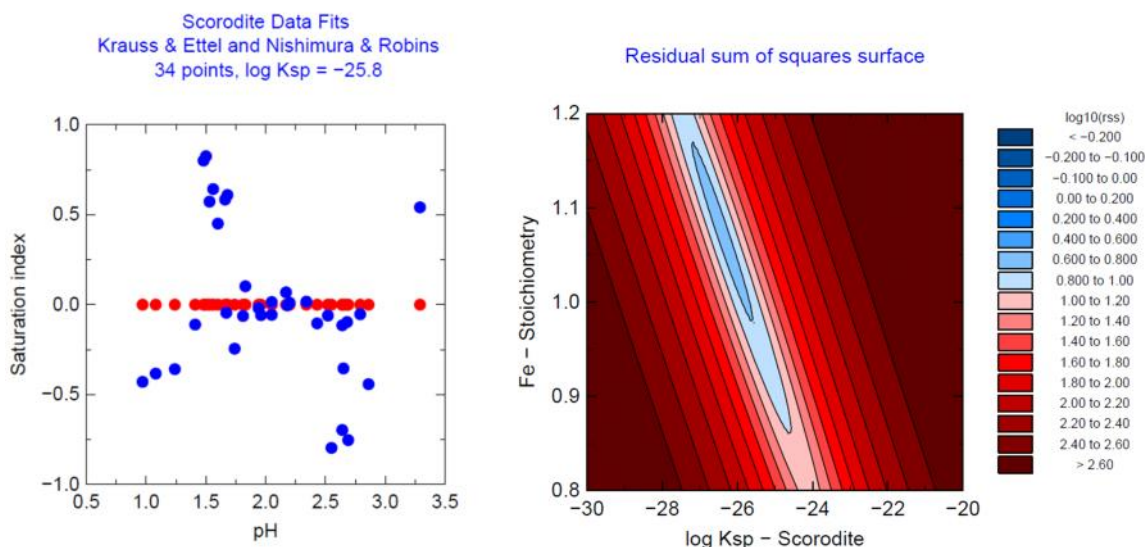
Uranyl Surface Complexation Species	Fitted $K_{int}$	Reaction	Method	Optimized Log K	Standard Deviation	No. of Observations/Data Sets
Strong Site Uranyl	$K_{1int}$	$Hfo\_sOH + UO_2^{+2} = Hfo\_sOUO_2^+ + H^+$	PHREEQC/UCODE_2005	3.792	$\pm 7.97E-01$	38/2 Strong and weak site complexes fit simultaneously
			PhreePlot	3.7897	$\pm 8.3788E-01$	
Weak Site Uranyl	$K_{2int}$	$Hfo\_wOH + UO_2^{+2} = Hfo\_wOUO_2^+ + H^+$	PHREEQC/UCODE_2005	2.507	$\pm 3.33E-01$	81/10
			PhreePlot	2.508	$\pm 3.4097E-01$	
Uranyl Monocarbonate	$K_{3int}$	$Hfo\_wOH + UO_2^{+2} + CO_3^{-2} = Hfo\_wOUO_2CO_3^- + H^+$	PHREEQC/UCODE_2005	9.150	$\pm 1.25E-01$	217/12
			PhreePlot	9.1474	$\pm 1.2389E-01$	
Uranyl Dicarbonate	$K_{4int}$	$Hfo\_wOH + UO_2^{+2} + 2CO_3^{-2} = Hfo\_wOUO_2(CO_3)_2^{-3} + H^+$	PHREEQC/UCODE_2005	15.28	$\pm 1.16E-01$	
			PhreePlot	15.2753	Not reported	

### SCORODITE AND YUKONITE SOLUBILITY DATA

PhreePlot was used as part of an effort to calculate the solubility product constant ( $K_{sp}$ ) and formula for yukonite, a calcium ferric arsenate, which may control arsenic concentrations under some conditions, has had various formulas reported in the literature. The first step was to determine if PhreePlot could provide a log  $K_{sp}$  value and a reasonable stoichiometry for a known phase. Scorodite ( $FeAsO_4 \cdot 2H_2O$ ) was selected for several reasons. Its formula is well defined and I had worked with the data set presented in Langmuir et al. (2006), and like yukonite it is also a ferric arsenate. In the 2006 paper, we used a trial and error method with a simple sum of the squared residuals to confirm the fits. As an exercise, a data set was used to verify the previously reported solubility product (log  $K_{sp}$ ) for crystalline scorodite. The data set contained 34 points. In the model, the log  $K_{sp}$  was adjusted to optimize the fit by minimizing the difference between the “observed” target saturation indices (SIs), which were set to zero, and having PhreePlot fit the SIs by adjusting the log  $K_{sp}$  value. These calculations can easily be conducted using just PHREEQC and averaging the saturation indices, but to accomplish further fittings using PhreePlot this step was required. PhreePlot uses tags, which are identified by less than and greater than symbols < > within the PHREEQC part of the file. For the initial setup only the <log\_k1> value changed.

```
Scorodite_fitted      405
FeAsO4:2H2O = Fe+3 + AsO4-3 + 2H2O
log_k                  <log_k1>
```

For crystalline scorodite, Langmuir et al. (2006) reported a log  $K_{sp}$  value of  $-25.83 \pm 0.07$ . For the PhreePlot calculations, the observation file defined the SIs for all samples at 0.00. This is different from calculations typically run using PhreePlot, where the measured data set shows the variance. In these calculations, the observed values (the SIs) were set to zero so there is no variance, but the experimental data do contain the variance, so the weighted residual sum of squares [W(RSS)] is still calculated. PhreePlot calculated log  $K_{sp}$  of  $-25.78 \pm 0.0724$  for crystalline scorodite. For the 34 data points, an average log  $K_{sp}$  calculated with PHREEQC was  $-25.774$  (Figure 1a).



**Figures 1a,b** PhreePlot prepared figure showing saturation indices as a function of pH. The “observed” values (red dots) are all set to zero. The blue dots represent the model calculated saturation indices after the program has adjusted the log  $K_{sp}$ . Figure (b) RHS, shows a contour plot showing the relationship between log  $K_{sp}$  and stoichiometric value for Fe

The next calculation was an effort to simultaneously calculate the log  $K_{sp}$  for scorodite and the stoichiometric coefficient for  $Fe^{+3}$ . This effort was a precursor to the yukonite calculations. To accomplish the second part of the fit the dissolution equation was redefined and the -no\_check option was included:



The relationship between <stoic1> and <stoic> was defined by the following numericTag:

$$\text{numericTags} \quad <stoic1> = 1.00 * <stoic>$$

The final estimates were close to the previous estimate with values of:

$$\log\_k1 = -26.40 \pm 0.34799, \text{ stoic} = 1.0739 \pm 0.040576$$

For such a large dataset a fit closer to 1.0 for the Fe stoichiometry was expected; the fit is somewhat disappointing. The contour plot is a feature in PhreePlot that helps refine optimization search strategies. Figure 1b shows the RSS as a function of log  $K_{sp}$  and Fe stoichiometry. A blue lens (valley) shows the strong relationship between the two variables, and without other data it would be difficult to further refine the result.

The subsequent yukonite modeling required the simultaneous fitting of up to four parameters (calcium, iron, arsenic and the solubility product constant). Data were provided by Dr. George Demopoulos and his students from McGill University.

The general formula for yukonite is  $\text{Ca}_x\text{Fe}_y(\text{AsO}_4)_z(\text{OH})_A$ , where A balances the charge according to:

$$A = 2.0 X + 3.0 \times Y - 3.0 \times Z$$

Due to convergence issues with the hydroxide term, most models were run using the Bound Optimization BY Quadratic Approximation (BOBYQA) method rather than the simpler Non-Linear Least Squares (NLLS). The BOBYQA method uses fitting parameter ranges. In one series of calculations, calcium was fixed at 2.0 and in the BOBYQA method the ferric and arsenate stoichiometries were allowed to vary within a small range. Both methods produced similar conclusions with a possible log  $K_{sp}$  near -111, and a formula of  $\text{Ca}_2\text{Fe}_3(\text{AsO}_4)_{3.03}(\text{OH})_{3.92}$  (Figure 2a), or -  $\text{Ca}_2\text{Fe}_3(\text{AsO}_4)_3(\text{OH})_4$ . Waters of hydration were not estimated. The room temperature results remain suspect; X-ray diffraction did not confirm yukonite in most of these samples. Furthermore, activities of the  $\text{Fe}^{+3}$  component show a large variation, which influences the calculations. A simulation using data from 75°C and confirmed to contain Yukonite produced a log  $K_{sp}$  of -119 and a formula of  $\text{Ca}_2\text{Fe}_3(\text{AsO}_4)_2(\text{OH})_7$ . The fit appears to be poorer than the room temperature fit. The discrepancy between the formulas and log  $K_{sp}$ 's and the visually poor fits for the data at 75°C (Figure 2b) raise questions about all the optimization results.

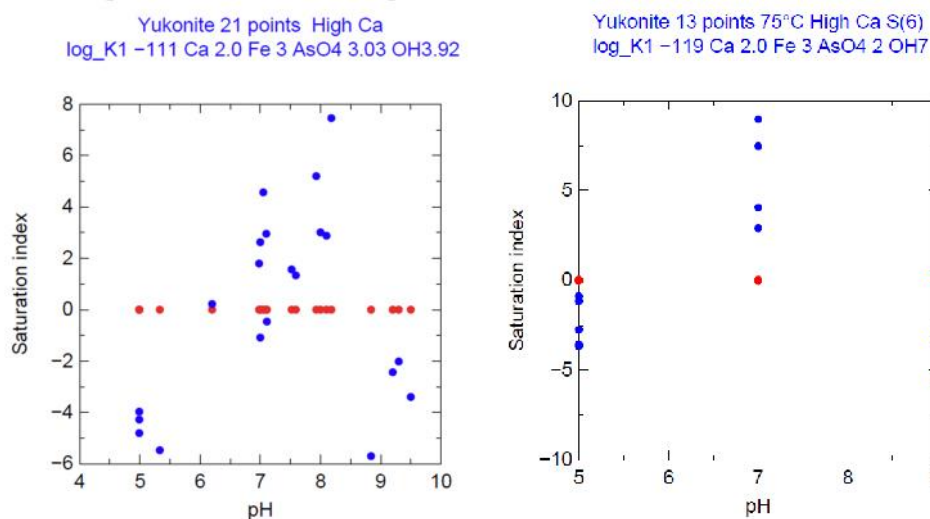


**Figure 2a, 2b** Example PhreePlot calculations to estimate Yukonite solubility. Figure 2a (left) shows the saturation indices for the 21 samples (blue dots) at room temperature after fitting, compared to “observed” values which were set to zero (red dots). Figure 2b (right) was for 13 samples run at 75°C.

Detailed contour plots based upon 52 data points were used to better define the relationship between the Fe and  $\text{AsO}_4$  stoichiometric proportions. PhreePlot sweeps through a defined range of reaction coefficient values, and using the activities of the components in the solutions and the assigned stoichiometries the program calculates a log  $K_{sp}$  value. Using the measured concentrations, PhreePlot then calculates a  $W(\text{RSS})$  and prepares contour plots of the  $\log_{10}(\text{rss})$  values. Numerous data sets were evaluated. Figures 3a and 3b show some of these results. Unlike the deep narrow valley shown for scorodite (Figure 1b) the yukonite figures indicate that there are large “flat” zones where the iron stoichiometric values, in particular, show a large degree of uncertainty. For the  $\text{Ca}_2\text{Fe}_y(\text{AsO}_4)_z(\text{OH})_a$  calculations for the oval that represents the minimum RSS (darkest blue), the

range for Fe is more than 2.0 units long, and even the As ranges from 1.65 to 2.65. To get a sense of how the Ion Activity Product (IAP) changes with changing stoichiometries, calculations were prepared using 1200 mg/L arsenic as arsenate, 1000 mg/L Ca, 2500 mg/L sulfate, the pH was fixed at 7.5 and ferrihydrite was present. These IAP values do not represent saturated conditions. “Yukonites” show a large spread in their log IAP values, for the upper point with Fe at 2.6 and AsO<sub>4</sub> at 2.4 (Figure 3a) the log IAP is -96.10. The smallest Fe value within the oval was Fe at 0.55 and AsO<sub>4</sub> at 1.65, and the log IAP value was -29.70. For the Ca<sub>3</sub>Fe<sub>y</sub>(AsO<sub>4</sub>)<sub>z</sub>(OH)<sub>a</sub> formulas (Figure 3b) the upper and lower IAP values were -126.16 and -44.61. These ranges are too great to develop unique formulas and log K<sub>sp</sub> values.

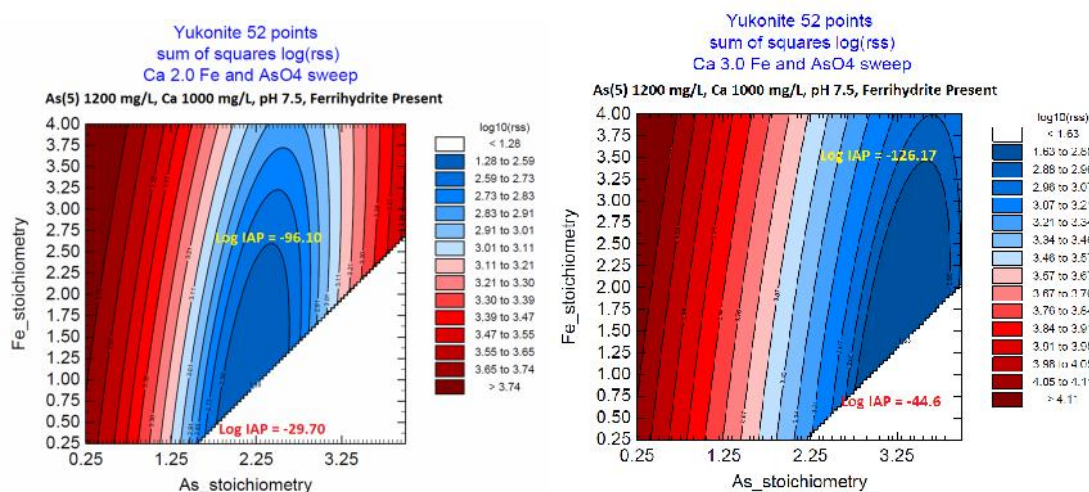


**Figure 3a, 3b** PhreePlot calculations used to evaluate stoichiometry factors for Fe and As for Yukonite. Figure 3a (left) used a Ca value of 2 and Figure 3b (right) used a Ca value of 3. White regions failed to converge in PHREEQC

Based upon the simpler scorodite calculation the approach appears to work, but it is highly sensitive to the quality of the data, and for yukonite the final parameter fit remains inconclusive at this time. It may be that ferric activities change as these samples age, further complicating the fitting calculations. This type of approach may be best for an iterative evaluation of laboratory data.

### CALCULATION OF SURFACE SITE CONCENTRATIONS

The ability to vary any parameter in a PHREEQC model, provided one has sufficient data, means that better geochemical models can be developed, tested and refined using PhreePlot. In preparing a surface water discharge model for a uranium mill Mahoney and Frey (2014) used PhreePlot in several ways to produce a more rigorous model. One example is shown below.

The surface discharge model performed a series of mixing calculations for each year’s discharge. The model is mainly a mixing model that uses site specific water balances to mix the various waters including surface waters and precipitation (rain and snow) at the discharge point. Additional surface water and precipitation dilute the composition in the two downstream lakes. The model was setup to allow for a wide range of options including evaporation, mineral precipitation and surface complexation. When appropriate, reactions in the receiving water bodies are included. Each model year was simulated independently. There was no year to year carry over in the models.

In the surface water discharge model, source waters are mixed at a discharge point (reservoir) and the waters flow through two additional bodies of water. By volume the two most important waters are from pit dewatering operations followed by the treated effluent from the mill. Chemical loads come from the treated mill water (Mill Discharge in Figure 4). For many major ions, simple mixing and dilution processes explain their concentrations in the downstream locations. However, arsenic concentrations are too low in the reservoir to be explained solely by mixing and dilution, so there must be an alternative geochemical process. Initial source term concentrations are too low for mineral solubility controls, so surface complexation becomes a means for arsenic attenuation. There is sufficient dissolved iron, particularly from the pit dewatering wells, that ferrihydrite appears to form and settle at the mixing/discharge point. Therefore, as part of the arsenic evaluation a surface complexation sub-model was included in the overall setup. Previous experience with arsenic surface complexation in pit lake models indicated that arsenic concentrations are unrealistically low when the standard site density parameter of 0.2 moles of weak HFO sites per mole of ferrihydrite precipitated is used. Therefore, it was decided to prepare a model that tracked the amount of HFO that formed as the waters were mixed at the discharge point, and then fit the surface site density to obtain the best fit for the arsenic in the three lakes. Twelve data points, each representing annual averages for the various source terms and the concentrations in the three lakes for a total of 36 points were used. Surface complexation constants reported in Gustafsson and Bhattacharya (2007) for arsenic were used instead of the values in Dzombak and Morel (1990), speciation reactions defined in Langmuir et al. (2006) and Marini and Accornero (2010) were included. Based upon other observations, it was decided to estimate two different site concentration values. The first one was for the first six years, followed by another estimate for the final six years. The calculations adjusted the <sitedens> value. For years 1 through 6 the PHREEQC input follows:

SURFACE 1012000

Hfo\_wOH Ferrihydrite equilibrium\_phase <sitedens> 53400

Hfo\_sOH Ferrihydrite equilibrium\_phase <Strong>

The lines of input shown above tell PHREEQC to define the weak site surface concentration Hfo\_wOH based upon the moles of ferrihydrite present as an equilibrium\_phase times the value of sitedens. The surface area is assumed to be 600 m<sup>2</sup>/g or 53400 m<sup>2</sup>/mole of Ferrihydrite present as the equilibrium\_phase. The strong site concentration Hfo\_sOH is defined in a similar manner, but the strong site value is related to the weak site concentration through the following numericTag, <Strong>="<sitedens>/40". A similar setup was used for years 7 through 12, but the terms were <sitedens2> and <Strong2>. As ferrihydrite only forms in the first lake it is also the only location where surface complexation takes place. The lowering of concentrations in lakes 2 and 3 is caused by dilution from surface waters and rainfall/snowfall.

The PhreePlot estimated site density values were:

$$\text{sitedens} = 9.0497\text{E-}02 \pm 1.7243\text{E-}02$$

$$\text{sitedens2} = 1.2961\text{E-}01 \pm 1.4404\text{E-}02$$

The site density values for the Hfo\_wOH sites are about half of the value originally defined in Dzombak and Morel (1990), they defined a value of 0.2 sites per mole of HFO precipitated for weak sites. The fitted model uses smaller values and is considered to be more conservative (i.e., protective of the environment). Figure 4 compares different model setups for arsenic. The figure

shows a mixing/dilution only scenario (purple circles) which clearly overestimates estimates arsenic concentrations. The red lines are the optimized arsenic modeled concentrations based upon the fitted site densities. Surface complexation also appears to influence uranium concentrations, but a problem was noted, the site density values when fitted to the arsenic data produced models that underestimate uranium surface complexation and overestimate uranium concentrations in the lakes. The differences between the arsenic and uranyl fits suggest a disconnect in the surface complexation databases. It was decided to retain these lower site density values because higher surface site concentrations would lower dissolved arsenic concentrations producing a less conservative model. Also, the values tend to predict somewhat high uranium concentrations, which are considered to produce a more conservative model.

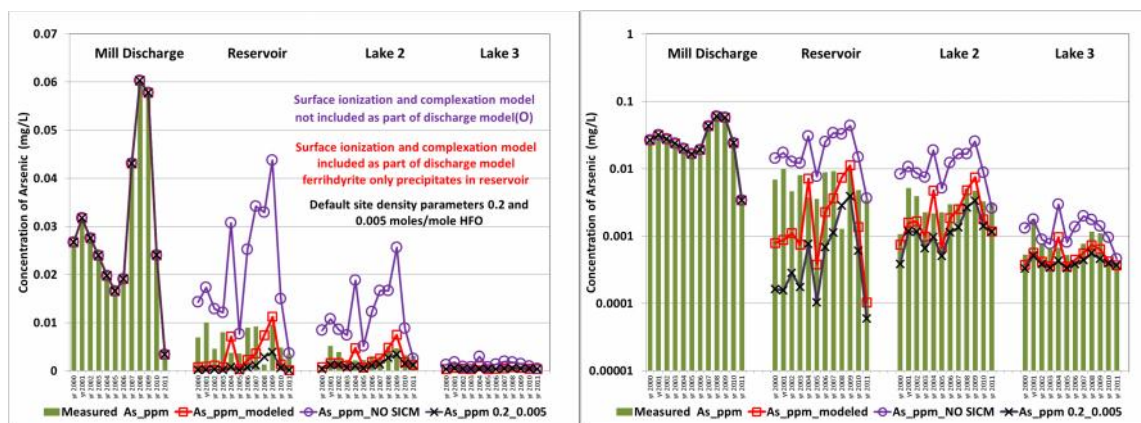


**Figure 4a, 4b** Surface water discharge model for arsenic, linear (a) and log concentrations (b). The figures shows observed values as green lines, the open circles did not include surface complexation reactions, red squares represent PhreePlot fitted model with surface complexation reactions on precipitated HFO. Black X's used the default site densities defined in Dzombak and Morel (1990)

### ESTIMATION OF RATE LAW CONSTANTS

The following example shows how laboratory leach tests can be used to optimize a parameter in a geochemical model. Rate constants for kinetic models can also be fit using PhreePlot. Leach amenability studies (also called bottle roll tests) were used to determine rate constants for uraninite (UO<sub>2</sub>) dissolution for a proposed in-situ uranium recovery operation in the Powder River Basin (Wyoming). The rates and rate law were subsequently included in a PHAST (Parkhurst et al. 2012) model to understand the nature of the leaching process in a three dimensional reactive transport system. The tests are used to demonstrate that the uranium mineralization is capable of being leached using conventional in-situ leach (ISL) methodologies. The leaching solution consisted of sodium bicarbonate (1 g/L NaHCO<sub>3</sub>) as the carbonate complexation agent. Hydrogen peroxide at 0.5 g/L H<sub>2</sub>O<sub>2</sub> (equivalent to 235 mg/L of dissolved oxygen) was used as the uranium-oxidizing agent. These tests were conducted at ambient pressure.

The bottle roll tests used 300 grams of solid and 1500 ml of leachate, the subsequent PHREEQC models maintained these proportions and used 200 grams of solid for 1 L of solution. The bottles were rolled for 16 hours (5.76e4 seconds), with eight hours available to collect samples and set up the next cycle, each sample under went six cycles. Ten tests were run and the ten samples covered a range of concentrations.

A kinetic model was developed to obtain a rate constant (k) for the dissolution of uraninite. A modified version of the rate law developed by Posey-Dowty et al. (1987) was used. The original rate law was:

$$dU/dt = k (SA/V)(O_2)^{0.5}((U_s - [U])/U_s)$$

Where: k is the rate constant at  $4.9(\pm 2.2)e-5$  (mole)(1)(m)<sup>-1</sup>(atm)<sup>-1/2</sup>(min<sup>-1</sup>) reported by Posey-Dowty et al., (1987). Converting to seconds the value is  $8.166 e-7$ (mole)(1)(m)<sup>-1</sup>(atm)<sup>-1/2</sup>(sec<sup>-1</sup>), and

- SA is surface area in m<sup>2</sup>,
- V is volume of water in liters,
- O<sub>2</sub> is the partial pressure of oxygen in solution in atmospheres,
- U<sub>s</sub> is the uranium concentration at saturation, and [U] is the concentration of uranium at that point in time (units are moles) in the model.

The original paper was vague in defining the  $(U_s-[U])/U_s$  term. They did not define the mineral that was to attain saturation or provide a limiting value for U<sub>s</sub>, so the rate law was changed to:

$$dU/dt = k (SA/V)(O_2)^{0.5}((1-SR("Schoepite"))*(m/m0)^{power}$$

SR is the saturation ratio ( $IAP/K_{eq}$ ), and the term  $((1-SR("Schoepite"))$  slows the overall dissolution rate as the solution approaches saturation with schoepite. This type of limiting term is commonly used in many PHREEQC rate laws. At equilibrium, the SR = 1.0 and the dissolution process halts. For these models, uraninite was originally considered as the limiting mineral, but leaching conditions were so far from saturation with uraninite, that the SR term is exceedingly small, and would not have any impact as dissolution proceeded. The m0 value represents the moles of uraninite at time 0.0, and m represents the number of moles as the dissolution process proceeds. The  $(m0/m)$  term provides a means to adjust the rate as the uraninite particles get smaller and the surface area decreases. For theoretical reasons, the term is usually raised to the 0.67 power, but better fits were noted in the models where the power was 1.0.

The preferred RATES keyword for uraninite dissolution written in BASIC is:

```
RATES; Uraninite; -start
10 if(si("Uraninite")>=0) then goto 50
15 if (m <= 0) then goto 50
20 rate=<Rate_constant>*parm(1)*((10^SI("O2(g)"))^0.5)*(1-
SR("Schoepite"))*(m/m0))
30 moles = rate * time
40 if (moles > m) then moles = m
50 save moles
-end
```

The model also required a surface area (SA/V) value and uraninite concentrations, i.e., the m0 terms for each sample. Laboratory data provided the uraninite concentrations and QEMSCAM data indicated that the average diameter of the uraninite particles was 20 microns. The particles were assumed to be spherical, the areas were calculated. These surface areas are the parm(1) term in each model.

The 2012 models were prepared using PHREEQC and the rate constant was estimated using a trial and error method. The fit was based upon the Test 8 results, which had the largest concentration of uranium. Each bottle roll test was modeled using a one cell six shift TRANSPORT model. Essentially, the "beaker" (or cell in PHREEQC syntax) contained 0.2 kilograms of solid sample and

contacted 1 liter of fresh leaching solution six times. The time for each contact was assumed to be 16 hours or 5.76e4 seconds. For the trial and error approach this provided the needed concentrations as a function of time. The rate constant was used to prepare models of the other nine tests and the observations were compared to the modeled values. The trial and error fits were acceptable. To get the sequence of data in the SELECTED\_OUTPUT file for the PhreePlot calculations, rather than use six shifts, an initial non-transport step was used, followed by five shifts in the TRANSPORT step, and the PRINT keyword turned writing to the SELECTED\_OUTPUT file off and on, as needed (D. Parkhurst, personal communication).

The earlier trial and error method produced a rate constant of  $2.8 \times 10^{-7} \text{ (mole)(l)(m)}^{-1} \text{ (atm)}^{-1/2} \text{ (sec)}^{-1}$ , the value was subsequently used in a PhreePlot calculation to estimate the W(RSS) and for the sixty data points, the W(RSS) was 1.5754e04. Two different models were run using PhreePlot. The first model used the  $(m/m_0)^{0.67}$  function (Figure 5) and the second model used a 1.0 power. A smaller W(RSS) was produced for the  $(m/m_0)^{1.0}$  model. This is probably because the uraninite particles are not all 20 micron spheres. The best fit value is  $2.433 \times 10^{-7} \pm 1.011 \times 10^{-8} \text{ (mole)(l)(m)}^{-1} \text{ (atm)}^{-1/2} \text{ (sec)}^{-1}$ . This value is close to the trial and error value estimates in 2012. Both rate constants are less than the value reported by Posey-Dowty et al. (1987). But differences are relatively small and could be related to differences in sample storage and handling, particle size estimates and subsequent estimation of surface areas, or differences between the two ore deposits.

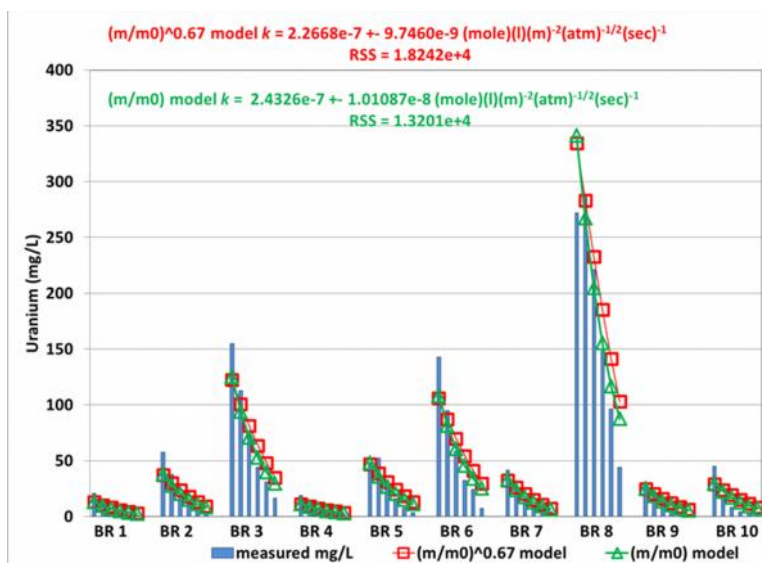


Figure 5 Bottle roll test data (blue lines) and PhreePlot Model fits. Red squares used an  $(m_0/m)^{0.67}$  term, green triangles used an  $(m_0/m)^{1.0}$  term

## CONCLUSIONS

Nearly any parameter in a PHREEQC model can be fit using PhreePlot to better match observational data and produce a better model. Potential future applications might include: adjusting mixing parameters in a pit lake model to match early recovery time concentration data in the nascent lake to further refine the water balance, or for a 1 dimensional transport model, the length of time for shifts in a series of cells can be fit to calibrate transport velocities by matching the concentrations observed over time in a down gradient well with the modelled estimates. Such

calibrations even with limited early data produce better long term predictive models. The surface water discharge model described previously demonstrates this process. An improved understanding of the role of different processes also provides further insights about the whole discharge operation, which further strengthens the “what if” scenarios that are typically considered in predictive models.

This paper has shown just a few applications of the fitting capabilities in PhreePlot. It is hoped that other users will continue to apply PhreePlot to their specific studies.

## REFERENCES

- Dzombak, D.A. and Morel, F.M.M., 1990. Surface complexation modelling: hydrous ferric oxide. Wiley-Interscience, New York, 393 p.
- Gustafsson, J.P., and Bhattacharya, P., 2007. Geochemical modeling of arsenic adsorption to oxide surfaces. (Chapter 6). *in* Arsenic in Soil and Groundwater Environment, P. Bhattacharya, A. B. Mukherjee, J. Bundschuh, R. Zevenhoven, R. H. Loeppert (Editors) Trace Metals and other Contaminants in the Environment, Volume 9, pp. 159–206 Elsevier B.V.
- Kinniburgh, D. G., and Cooper, D. M., 2004. Predominance and mineral stability diagrams revisited. *Environ. Sci. Technol.* v. 38, No.13, pp. 3641-3648.
- Kinniburgh, D. G., and Cooper, D. M., 2011. PhreePlot – Creating graphical output with PHREEQC. Available at <http://www.phreeplot.org/>, original date June 2011, last updated December 17, 2014, 606 p.
- Langmuir, D., Mahoney, J., and Rowson, J., 2006. Solubility products of amorphous ferric arsenate and crystalline scorodite (FeAsO<sub>4</sub>·2H<sub>2</sub>O) and their application to arsenic behavior in buried mine tailings: *Geochimica et Cosmochimica Acta.*, vol. 70, pp. 2942-2956.
- Mahoney, J.J., Cadle, S.A., and Jakubowski, R.T., 2009. Uranyl adsorption onto hydrous ferric oxide – a re-evaluation for the diffuse layer model database. *Environ. Sci. and Technol.*, v. 43, no. 24, pp. 9260-9266. DOI 10.1021/es901586w.
- Mahoney, J.J., and Frey, R.A., 2014. Calibration of a PHREEQC Based Geochemical Model to Predict Surface Water Discharge Compositions from an Operating Uranium Mill in the Athabasca Basin. Presented at URAM 2014, Material for the Nuclear Fuel Cycle: Exploration, Mining, Production, Supply and Demand, Economics and Environmental Issues. IAEA. Vienna, Austria. (in press).
- Marini, L., and Accornero, M., 2010. Erratum to: Prediction of the thermodynamic properties of metal–arsenate and metal–arsenite aqueous complexes to high temperatures and pressures and some geological consequences. *Environ. Earth Sci.* Vol. 59, pp. 1601-1606.
- Parkhurst, D.L., and Appelo, C.A.J., 2013. Description of input and examples for PHREEQC version 3 – A computer program for speciation, batch-reaction, one-dimensional transport, and inverse geochemical calculations: U.S. Geological Survey Techniques and Methods, book 6, chap. A43, 497 p., available only at <http://pubs.usgs.gov/tm/06/a43>.
- Parkhurst, D.L., Kipp, K.L., and Charlton, S.R., 2010. PHAST Version 2 – A program for simulating groundwater flow, solute transport, and multicomponent geochemical reactions: U.S. Geological Survey Techniques and Methods 6–A35, 235 p.
- Poeter, E. P., Hill, M. C., Banta, E. R., Mehl, S., Christensen, S., 2005. UCODE\_2005 and Six Other Computer Codes for Universal Sensitivity Analysis, Calibration and Uncertainty Evaluation; Techniques and Methods 6-A11; USGS: Reston, VA.
- Posey-Dowty, J., Axtmann, E., Crerar, D., Borcsik, M., Ronk, A., and Woods, W. 1987. Dissolution rate of uraninite and uranium roll-front ores. *Economic Geology*, Vol. 82, pp. 1493 -1506.